

## **On the Temporal-spatial Analysis of Estimating Urban Traffic Patterns Via GPS Trace Data of Car-hailing Vehicles**

Jiannan Mao <sup>a, b</sup> Lan Liu <sup>a</sup>, Hao Huang <sup>a</sup>, Weike Lu <sup>c, d</sup>, Kaiyu Yang <sup>a</sup>, Tianli Tang <sup>e</sup>,  
and Haotian Shi <sup>b\*</sup>

*<sup>a</sup> School of Transportation and Logistics, Southwest Jiaotong University, Chengdu, China;*

*<sup>b</sup> Department of Civil and Environmental Engineering, University of Wisconsin-Madison,  
Madison, United States of America;*

*<sup>c</sup> School of Rail Transportation, Soochow University, Soochow, China;*

*<sup>d</sup> Alabama Transportation Institute, Tuscaloosa, United States of America;*

*<sup>e</sup> School of Transportation, Southeast University, Nanjing, China;*

\*Corresponding author: Haotian Shi, Department of Civil and Environmental Engineering,  
University of Wisconsin-Madison, 1217 Engineering Hall 1415 Engineering Drive, Madison,  
WI, United States of America, 53705, e-mail: hshi84@wisc.edu

Word count = 6985 words

## **On the Temporal-spatial Analysis of Estimating Urban Traffic Patterns Via GPS Trace Data of Car-hailing Vehicles**

### **Abstract**

Car-hailing services have become a prominent data source for urban traffic studies. Extracting useful information from car-hailing trace data is essential for effective traffic management, while discrepancies between car-hailing vehicles and urban traffic should be considered. This paper proposes a generic framework for estimating and analyzing urban traffic patterns using car-hailing trace data. The framework consists of three layers: the data layer, the interactive software layer, and the processing method layer. By pre-processing car-hailing GPS trace data with operations such as data cutting, map matching, and trace correction, the framework generates tensor matrices that estimate traffic patterns for car-hailing vehicle flow and average road speed. An analysis block based on these matrices examines the relationships and differences between car-hailing vehicles and urban traffic patterns, which have been overlooked in previous research. Experimental results demonstrate the effectiveness of the proposed framework in examining temporal-spatial patterns of car-hailing vehicles and urban traffic. For temporal analysis, urban road traffic displays a bimodal characteristic while car-hailing flow exhibits a ‘multi-peak’ pattern, fluctuating significantly during holidays and thus generating a hierarchical structure. For spatial analysis, the heat maps generated from the matrices exhibit certain discrepancies, but the spatial distribution of hotspots and vehicle aggregation areas remains similar.

**Keywords:** Intelligent Transportation Systems; Car-hailing; GPS trace data; Temporal and spatial distribution;

## 1. Introduction

Urban traffic patterns embody the intricate and dynamic interplay between vehicular movements and human activities within road networks. Understanding and accurately estimating these patterns can substantially enhance traffic efficiency, safety, and sustainability in urban areas (Correa & Ozbay, 2022). Recent advancements in communication technology and fundamental infrastructure have facilitated the acquisition of Global Positioning System (GPS) data from Intelligent Traffic Systems (ITS) (Qian et al., 2021; J. Yu et al., 2020; Zhong et al., 2016). These supply traffic management and control systems with a more comprehensive understanding of vehicle trajectories compared to conventional sensor data (D'Andrea & Marcelloni, 2017; He et al., 2019; Liu et al., 2022). In particular, GPS trace data can be employed to estimate urban traffic patterns effectively (Herrera et al., 2010). Consequently, extracting valuable spatial-temporal information from GPS trace data and analyzing traffic patterns derived from such data has become a topic of considerable academic importance.

GPS data can be collected via vehicle onboard units or mobile phone data to illustrate vehicle movements (Tu et al., 2021). Mining the GPS data can extract traffic metrics (e.g., traffic speed and flow) and then analyze pertinent information, such as temporal distribution patterns and spatial aggregation states of traffic (Yuan et al., 2021; Zheng, 2015). In this domain, prior research has employed GPS trace data for various purposes. For example, Moreira et al. (Moreira-Matias et al., 2013) predicted the spatial distribution of taxi passengers using taxi GPS traces to devise a more intelligent taxi dispatching strategy. Studies (An et al., 2018; An et al., 2016) identified recurring congestion evolution patterns by employing grid divisions and GPS-equipped vehicle mobility data. D'Andrea et al. (D'Andrea & Marcelloni, 2017) introduced an expert system for detecting traffic congestion and incidents using real-time GPS data from GPS trackers or drivers' smartphones. Several studies have also integrated trace data with traffic flow theories to examine traffic patterns. For instance, using GPS data, Wang et al. (Wang Yu et al., 2022) developed a comprehensive model incorporating a real-time lane identification model and a real-time queue length estimation model based on traffic shockwave theory. Similarly, Tu et al. (Tu et al., 2021) combined three-phase traffic flow theory and presented a framework to categorize traffic flow states, which can process massive, high-density, and noise-contaminated smartphone sensor data sets.

Although the wealth of trace data has profoundly influenced numerous studies in the traffic

domain, significant challenges persist in utilizing vehicle trajectory data for traffic estimation tasks. Specifically, some GPS traces may only contain the latitude and longitude of each point without instantaneous velocity, necessitating additional processing and supplementary data sources, as demonstrated in previous studies (Herrera et al., 2010; Liu et al., 2020; Tu et al., 2021; J. Yu et al., 2020; Wenhao Yu, 2018). Moreover, some coarse-grained algorithms, primarily designed for business applications, may not be suitable for road-based estimation tasks since they partition urban networks into grids and allocate different traces to each grid (An et al., 2018; An et al., 2016; Liu et al., 2020; Wenhao Yu, 2018). Consequently, it is crucial to develop a practical road-level traffic pattern estimation framework capable of addressing incomplete data, such as data without instantaneous speed measurements.

Additionally, recent studies have focused on developing specialized approaches for distinct technical domains using GPS data, such as map-matching (D'Andrea & Marcelloni, 2017), semantic information interpretation (Al-Dohuki et al., 2016; Liu et al., 2020), and incomplete matrix completion (Chen et al., 2019; J. Yu et al., 2020). Although these methods have undeniably proven effective in addressing specific needs and requirements, there remains an urgent demand for a comprehensive and concise framework to handle road traffic estimation tasks. Hence, a general and user-friendly pre-processing estimation framework is needed to support academic research and practical traffic management. Such a framework will enable researchers and practitioners to effectively analyze and interpret large amounts of GPS trace data and extract valuable insights to support traffic management and control strategies.

In addition to addressing traffic estimation concerns (Correa & Ozbay, 2022; Xing et al., 2022), a generic framework is also desirable to connect potential applications in academia and car-hailing service providers (e.g., Uber, Lyft, and DiDi). How can academic researchers conveniently utilize the data provided by car-hailing service companies to generate urban traffic estimations? And how can car-hailing service providers benefit from the academic outputs cost-effectively? It is essential to consider the trade-off between business usage and academic research, and accommodate the needs of both parties. By tackling these challenges, the proposed estimation and analysis framework can foster collaborations between academia and industry, promoting the development of innovative solutions to address the complex challenges of urban traffic management.

## **2. Research goal and objectives**

With the above considerations, this paper proposes a generic traffic pattern estimation and analysis

framework utilizing car-hailing vehicle traces. The proposed estimation framework comprises three layers: the data layer, the software interaction layer, and the processing method layer. The data layer is designed to accommodate car-hailing trajectory data, while the software interaction layer integrates Python<sup>1</sup>, Open Street Map (OSM)<sup>2</sup>, and ArcGIS<sup>3</sup> to jointly process trace data and network information data. The processing method layer employs two types of data processing techniques: map correcting techniques, such as map-matching and trace corrective action, and data pre-processing techniques, such as data cutting and traffic measurement calculation. The estimation framework can be easily implemented with minimal software and data source requirements and can be further adapted to suit the evolving needs of various applications.

Next, we evaluate the performance of the proposed estimation-analysis framework using real-world car-hailing data. With car-hailing trace data as input, the car-hailing vehicle flow and the mean speed of road segments are calculated every fifteen minutes. The INRIX index (Dong et al., 2019; Reed, 2019), a widely used measure of road congestion levels, is chosen to assess the congestion level of roads. On this basis, we conduct comprehensive analyses of the temporal-spatial patterns of car-hailing vehicles and urban traffic, elucidating the relationships and differences between the two traffic modes. These analyses not only enhance the understanding of the two traffic patterns but also provide insights into the potential applications of the differences between them.

In summary, the main contributions of this paper are in three aspects. (i) We propose a generic traffic estimation framework that is applicable to a wide range of practical situations. Using car-hailing trace data, the estimation framework can effectively generate car-hailing flow and urban traffic speed matrices at the road level, which caters to further fine-grained transportation management and academic studies. (ii) The analysis block of the framework can help uncover the relationships between car-hailing vehicles and urban traffic patterns (i.e., correlations and differences) by comparing their temporal-spatial attributes, further contributing to car-hailing service management applications. (iii) We examine the pattern disparities between car-hailing vehicles and urban traffic, which have been largely overlooked in previous research. This oversight can potentially lead to flawed assessments of urban traffic when relying solely on data derived from car-hailing services.

---

<sup>1</sup> <https://www.python.org>

<sup>2</sup> <https://www.openstreetmap.org/>

<sup>3</sup> <https://developers.arcgis.com>

The rest of this paper is organized as follows: Section 3 introduces the specific content of the estimation-analysis framework and evaluation metrics; Section 4 shows real-world experimental results based on car-hailing data from Chengdu, China. Section 5 illustrates temporal and spatial distribution patterns derived from traffic speed and car-hailing vehicle flow, respectively; Section 6 discusses the difference between car-hailing vehicles and urban traffic flow; Section 7 concludes the findings and introduces future works.

### **3. Methodology**

#### ***3.1 Technical architecture***

Based on the objectives discussed in Section 2, this study aims to: (i) estimate car-hailing vehicle flow and urban road speed simultaneously using GPS data of car-hailing vehicles, and (ii) analyze temporal-spatial patterns of car-hailing service and urban traffic, particularly disparities in these two patterns.

To achieve the objectives, we develop a three-layer traffic pattern estimation framework for GPS trace data and incorporate an additional analysis block for assessing traffic patterns of car-hailing vehicles and urban traffic, as illustrated in [Figure 1](#). Specifically, the estimation framework comprises three primary layers: the data layer for standardizing the input data, the interactive software layer for establishing an underlying software foundation, and the processing method layer for handling pre-processing and estimating tasks. An analysis block is built upon the estimation results to examine the temporal-spatial patterns of car-hailing services and urban traffic vehicles. It is important to note that the processing method layer serves as a functional layer that closely interacts with the other two layers. Details of each layer will be discussed in the subsequent subsections.

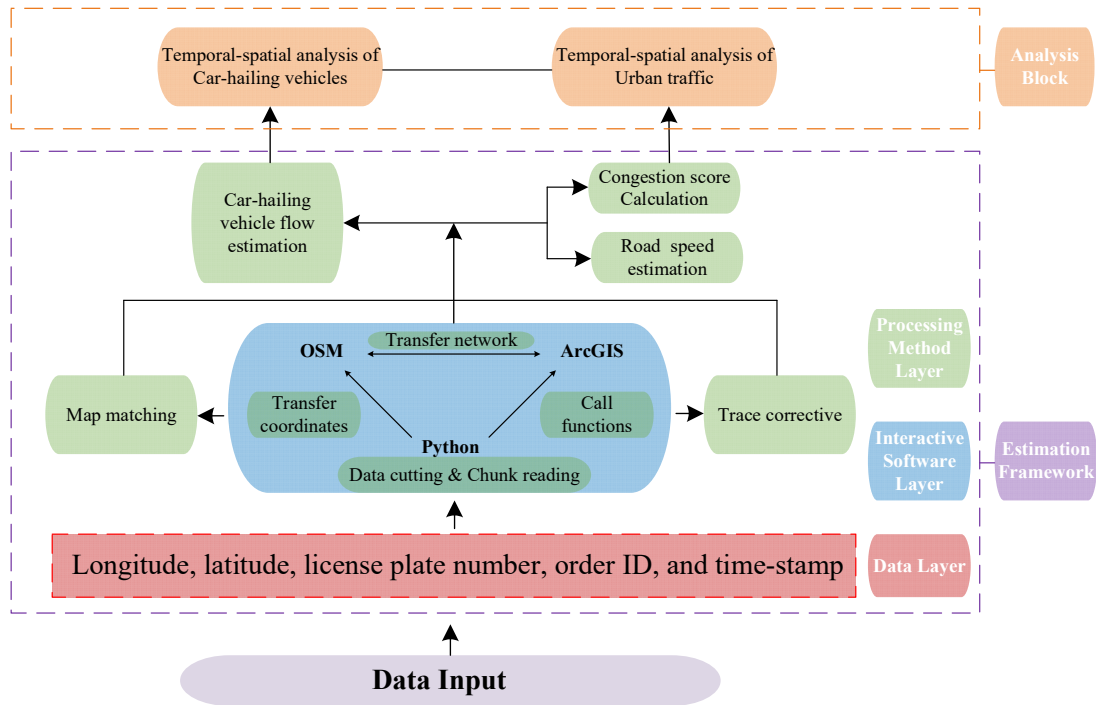


**Figure 1.** Flow chart of the estimation framework and analysis block

### 3.2 Data layer and interactive software layer

The data structure in this data layer should contain the longitude, latitude, license plate number, order ID, and time stamp of each point. For large-scale urban networks, the daily data magnitude will be in gigabytes (GB), which requires an efficient data reading and processing technique. Regarding the software interaction layer, we utilize Python, OSM, and ArcGIS to handle data processing and network structure representation.

These two layers aim to build a data and software environment for subsequent processing. For efficient data reading, chunk reading with a size of 10,000 is chosen to add data to files. Chunk reading can handle car-hailing data at an urban scale, as most car-hailing trace data, in reality, is in the GB magnitude. In terms of terabytes (TB) or larger data magnitude, Hadoop<sup>1</sup> can effectively accomplish the task. Regarding road map illustration and map matching of trace data, OSM can provide abundant urban network data, serving as a map base in ArcGIS.

### 3.3 Processing method layer

The processing method layer is an essential part of the traffic pattern estimation framework, responsible for the necessary processing techniques and methods required for pre-processing data

<sup>1</sup> <https://hadoop.apache.org/>

and map-matching operations. Specifically, its functions include data cutting, ArcGIS operation, car-hailing vehicle flow estimation, road average speed estimation, and congestion score calculation. This layer aims to transform raw data into relevant speed and flow tensor matrices for the temporal-spatial distribution analysis. The functions of each component are as follows:

### *3.3.1 Data cutting*

The first function of the processing method layer is data cutting, which involves transferring the read data to facilitate loading. As mentioned in Section 3.2, data is loaded using a chunk reading size of 10,000, and a sampling interval of fifteen minutes is set to divide the read data into sample pieces. The purpose of this function is to minimize memory usage and provide a database for illustration and analysis. In general, trace data can vary for a long period, and a sampling interval of fifteen minutes is sufficient for depicting the traffic evolution in urban road networks.

### *3.3.2 ArcGIS operation*

The ArcGIS operation is utilized for trace correction and map-matching. Initially, a fifteen-minute sample is selected to correct the divergence between tracepoints and the OSM map, which uses the default WGS-84 coordinate system. The ‘Near\_Analysis’ function of ArcMap, a combination tool of ArcGIS and Python, is employed to conduct a near-neighbor analysis based on the trace correction results. This function maps the trajectory points to roads with the shortest distances and labels the points with NEAR\_FID for the corresponding road ID.

Despite more advanced trace-correction and map-matching techniques that could potentially yield higher accuracy, the functions offered by ArcGIS and ArcMap enable users to tackle trace-correction and map-matching challenges with adequate precision that is suitable for engineering-focused applications.

### *3.3.3 Car-hailing vehicle flow and road speed estimation*

One aspect of our estimation process focuses on determining the flow of car-hailing vehicles. We achieve this by utilizing a fifteen-minute sample interval, which results in a tensor matrix containing the estimated number of car-hailing vehicles per road segment for each sample interval. Generally, each car-hailing order rarely passes the same road section twice within a short period due to the factors such as fuel cost and profit optimization. Consequently, the car-hailing vehicle flow estimation is approximated by counting the order IDs of different car-hailing vehicles that accumulate on each road segment during each sample interval.

Another aspect of the estimation process involves estimating the average speed of road



sections using car-hailing vehicles as indirect indicators. The underlying principle is that the average speed of a road section can be indirectly inferred from car-hailing vehicles that travel through it during a specified sample period. As a result, the calculation procedure can be structured as follows. First, pick out different traces according to order IDs and sort the points in each trace in terms of time stamps; Then, the average speed can be viewed as the ratio of the nearest distance (calculated by latitude and longitude of trajectory points) to the difference of time-stamp. Detailed calculation steps are listed below:

First, the Haversine formula (Gade, 2010) is employed to compute the distance  $d$  between any pair of longitude and latitude points as follows:

$$d_{r_{ij} \subset r_k} = 2r \arcsin \left( \sqrt{\sin^2 \left( \frac{\varphi_j^{lat} - \varphi_i^{lat}}{2} \right) + \cos \varphi_i^{lat} \cdot \cos \varphi_j^{lat} \cdot \sin^2 \left( \frac{\lambda_j^{lon} - \lambda_i^{lon}}{2} \right)} \right) \quad (1)$$

where,  $d_{r_{ij} \subset r_k}$  is the distance of the nearest trace pair  $r_{ij}$ , i.e., the distance between two nearest points  $i$  and  $j$  of the same GPS trace;  $r_k$  denotes the nearest GPS trace pair set that is located on road  $k$ , and  $r_{ij} \subset r_k$ ;  $r$  is the radius of the sphere (in this work, the approximate radius of the earth, 6378.137 km);  $\varphi_i^{lat}$  and  $\varphi_j^{lat}$  are the latitude of GPS trace points  $i$  and  $j$ , respectively; Analogous,  $\lambda_i^{lon}$  and  $\lambda_j^{lon}$  are the longitude of GPS trace points  $i$  and  $j$ , respectively.

Then the velocity of the trace point  $r_{ij}$  during the sample period  $\Delta t_{ij}$  (the sample period is chosen according to time stamps of the nearest two points with a threshold of 10 seconds) can be computed as follows:

$$v_{r_{ij} \subset r_k}^{\Delta t_{ij}} = \frac{d_{r_{ij} \subset r_k}}{\Delta t_{ij}} \quad (2)$$

where  $v_{r_{ij} \subset r_k}^{\Delta t_{ij}}$  is the velocity of the trace pair  $r_{ij}$ .

Based on Eq.(1) and Eq. (2), the average speed of road  $k$  can be obtained by computing the arithmetic mean of velocities of trace GPS trace pair set  $r_k$  as follows:

$$\bar{v}_{r_k} = \frac{1}{n(k)} \sum_{1}^{n(k)} v_{r_{ij} \subset r_k}^{\Delta t_{ij}} = \frac{1}{n(k)} \sum_{1}^{n(k)} \frac{d_{r_{ij} \subset r_k}}{\Delta t_{ij}} \quad (3)$$

where  $\bar{v}_{r_k}$  is the average speed of road  $k$ ;  $n(k)$  is the total number of nearest GPS trace pairs that belong to road  $k$ ; Note that the road speed is set to 0 when there is no GPS trace during the sample period.

This framework generally provides a straightforward yet effective method for estimating the car-hailing vehicle flow and road speed. While more sophisticated estimation methods may exist, our framework focuses on achieving computational efficiency and relatively high accuracy. As such, our framework serves as a practical solution for engineering-driven tasks.

### 3.4 Analysis block

The analysis block conducts temporal-spatial analyses for both car-hailing vehicles and urban traffic. It investigates their temporal and spatial dynamics (e.g., temporal patterns and spatial distribution) and compares their characteristics and potential implications.

Modifying the estimated traffic speed matrix is necessary for the temporal-spatial analysis of urban traffic, given the variability of traffic speeds across different roads. One straightforward way to present the traffic state is to evaluate traffic congestion on the same scale. Current studies on evaluating congestion rely mostly on V/C ratio, time delay, and congestion durations, which use metrics such as Travel Time Index (TTI) (Lasley, 2021; Lyman & Bertini, 2008) and LaneMile Duration Index (LMDI) (Rao & Rao, 2012). In this work, to simplify the evaluation process, we measure the congestion level solely based on the average road speed estimated by GPS traces. Therefore, we adopt INRIX index (Reed, 2019), which assesses the congestion degree of roads by average road speed, where a lower score indicates a better condition. The INRIX index measures congestion values by using the actual and free-flow speed of a certain road section, according to the following formula:

$$\text{INRIX}_{kl} = \begin{cases} \left( \frac{\text{TH}_k}{\text{RE}_{kl}} - 1 \right), & \left( \frac{\text{TH}_k}{\text{RE}_{kl}} - 1 \right) > 0 \\ 0, & \left( \frac{\text{TH}_k}{\text{RE}_{kl}} - 1 \right) \leq 0 \end{cases} \quad (4)$$

where,  $\text{INRIX}_{kl}$  is the congestion score of the road  $k$  during the  $l$ -th sample interval;  $\text{TH}_k$  is the free flow speed of road  $k$ ;  $\text{RE}_{kl}$  is the average actual speed of road  $k$  during the  $l$ -th sample interval.

When evaluating network-wide congestion levels, a weighted calculation can be applied as follows:

$$\text{INRIX}_l = \frac{\sum L_k \times \text{INRIX}_{kl}}{\sum L_k} \quad (5)$$

where,  $\text{INRIX}_l$  is the network congestion score during the  $l$ -th sample interval;  $L_k$  denotes the length of road  $k$ .

## 4. Experimental settings and processing

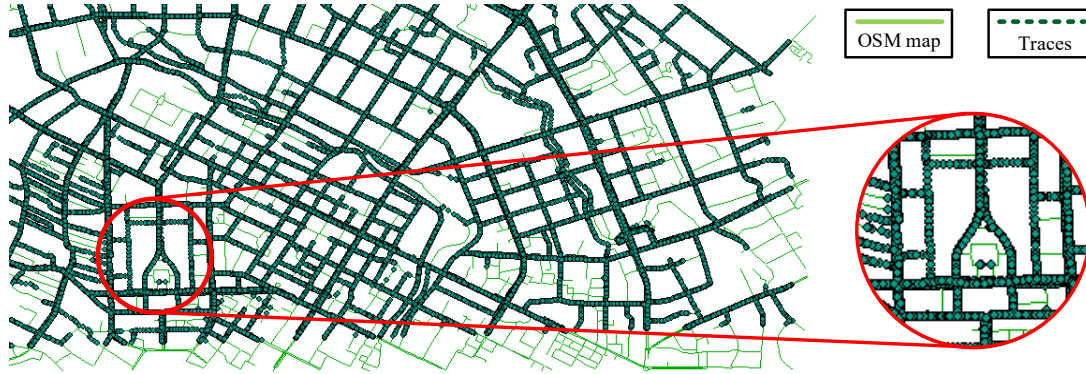
### 4.1 Experimental settings, trace correction, and map-matching

This section presents the experiment setting for evaluating the proposed three-layer estimation framework and analysis block, using anonymous car-hailing trace data from a part of Chengdu, China. The study area contains the central CBD of Chengdu city and is about 59.5 km<sup>2</sup>. The records include 30 days of car-hailing vehicle traces from October 1<sup>st</sup> to October 30<sup>th</sup>, 2016, with approximately 40 million daily trace records.

The car-hailing trajectory points were adjusted to suit the OSM map coordinates using ArcGIS operations. The result of a specific part of the experimental region is shown in Figure 2. The light green lines represent the base map obtained from OSM with the WGS-84 coordinate system, while the dark green points are the car-hailing trajectory points. An amplified of the city center is presented for a clear comparison. As shown in Figure 2(a), the original traces and OSM base map deviate but can be recovered by a shift in the northwest direction, as indicated by a yellow arrow. Then the basic ArcGIS operations are carried out to rectify trajectory points. As shown in Figure 2(b), it is clear that the operation is sufficient for correcting the shift.



(a) Before correcting. The yellow arrow denotes the correction operation direction.



(b) After correcting. Traces overlap well with the base OSM map.

**Figure 2.** Corrective operation with car-hailing trajectory points and the OSM map,

#### 4.2 Estimation process and data clean

Using our estimation framework, GPS trajectory data can be converted into two tensor matrices, each of which has the shape of about 2,000 roads and 2,880 time-stamps. Besides, the mean speed matrix requires further data pre-processing because the road speed data may only be collected when a road order record exists. As the study area is the central part of Chengdu city, it stands to reason that a busy central area in a large modern city will be the hotspot for car-hailing services. Therefore, we believe that removing those roads with a high fraction of missing values will have little effect on analyzing urban traffic patterns. Here, we set a threshold of 0.2 to filter missing values, and about 1,000 roads left. A simple linear interpolation is used to complement the rest data with the small number of missing values.

#### 4.3 Degree of congestion (DC) and car-hailing flow (CF)

As described in the methodology section, we employ the INRIX scores derived from the speed tensor matrix to measure the degree of traffic congestion (DC) which is a dimensionless measurement in the range of [0,1]. The car-hailing service is measured by car-hailing vehicle flow (CF), denoting the number of car-hailing vehicles per sample period. For a clear comparison version, the network-scale mean value of DC and the total value of CF on roads are computed as network-wide measurements. Then, we employ a fitting index  $f^2$  to quantify the dispersion degree of data. The fitting index can be computed as follows:

$$f^2 = 1 - \frac{\sum_{j=1}^n (y_j - \bar{y}_j)^2}{\sum_{j=1}^n (y_j - \bar{Y})^2} \quad (6)$$

where,  $y_j$  is the actual network-wide value (flow/speed) of sample interval  $j$ ;  $\bar{y}_j$  is the mean of all actual values during sample interval  $j$ ;  $\bar{Y}$  denotes the mean value of all  $n$  sample intervals; The closer  $f^2$  is to 1, the greater the number of values aggregated together, indicating that traffic state patterns are similar each day.

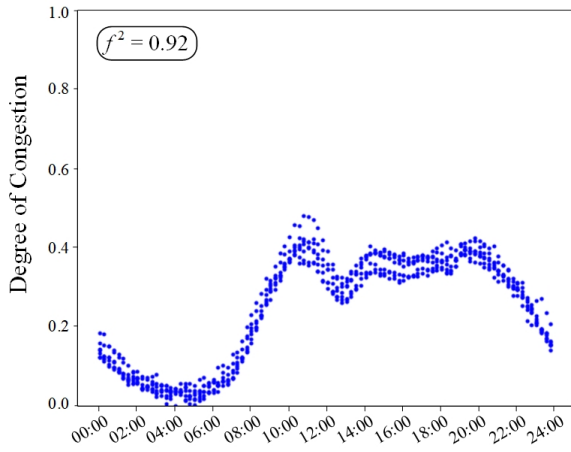
It should be noted that the arithmetic mean of instantaneous GPS speed can reflect the whole traffic condition of the road section, while the car-hailing vehicle flow only stands for car-hailing vehicle service. Thus it is possible to mine the relationship between car-hailing vehicles and urban traffic patterns by comparing the two measurements, DC & CF.

## 5. Temporal-spatial pattern analysis

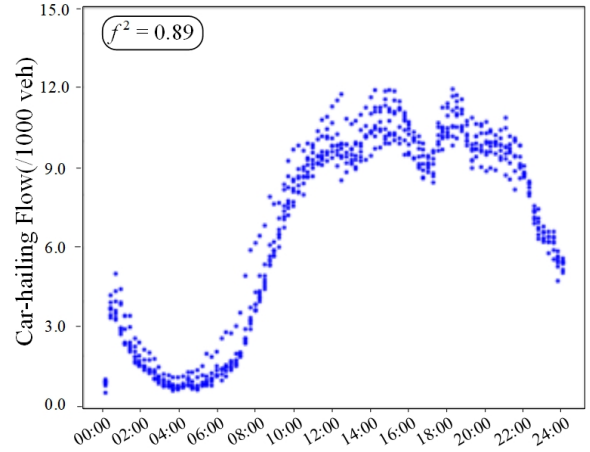
Analyzing temporal-spatial traffic patterns is essential for comprehending how traffic evolves and propagates over time and space (Deng et al., 2021). The following subsections will conduct temporal and spatial pattern analyses based on the CF of car-hailing service and DC of road traffic obtained from our estimation framework. By examining these patterns, we aim to uncover the inherent correlations between car-hailing services and urban road traffic, which can provide valuable insights into urban traffic dynamics.

### 5.1 Temporal pattern analysis

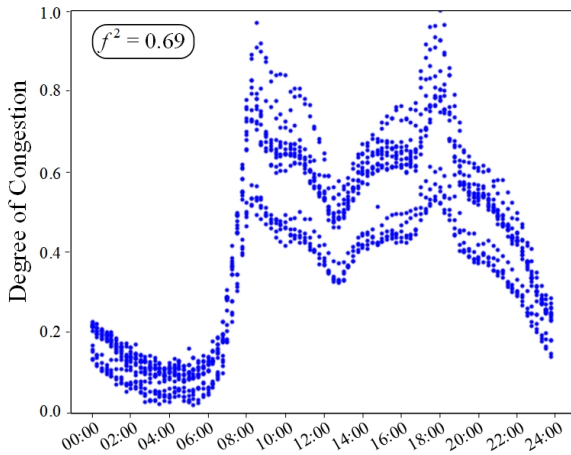
This section analyzes temporal patterns of car-hailing vehicles and road section traffic, and comparisons will be made to excavate the relationship between them. The DC (INRIX scores, representing speed) and CF for each sample interval are plotted in Figure 3. The chosen data period includes a seven-day holiday (the National Day of China, from October 1<sup>st</sup> to October 7<sup>th</sup>). In Figure 3, each blue point represents the network-wide value every fifteen minutes. The x-axis represents the time of day, while the y-axis denotes the DC/CF values. The sub-plots, Figure 3(a-c), illustrate the DC, whereas sub-plots, Figure 3(d-f), depict the CF.



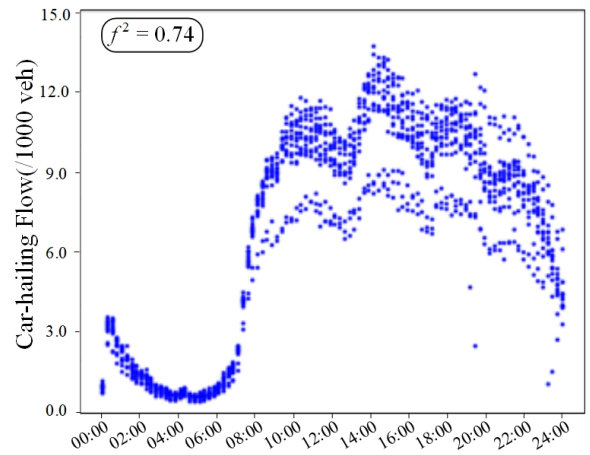
(a) National Day (DC)



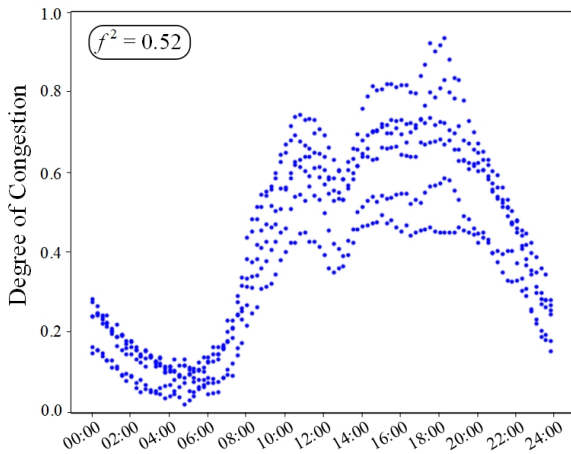
(d) National Day (CF)



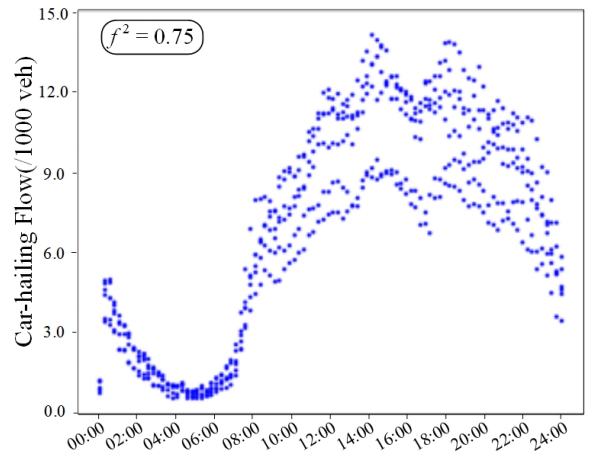
(b) Weekday (DC)



(e) Weekday (CF)



(c) Weekend (DC)

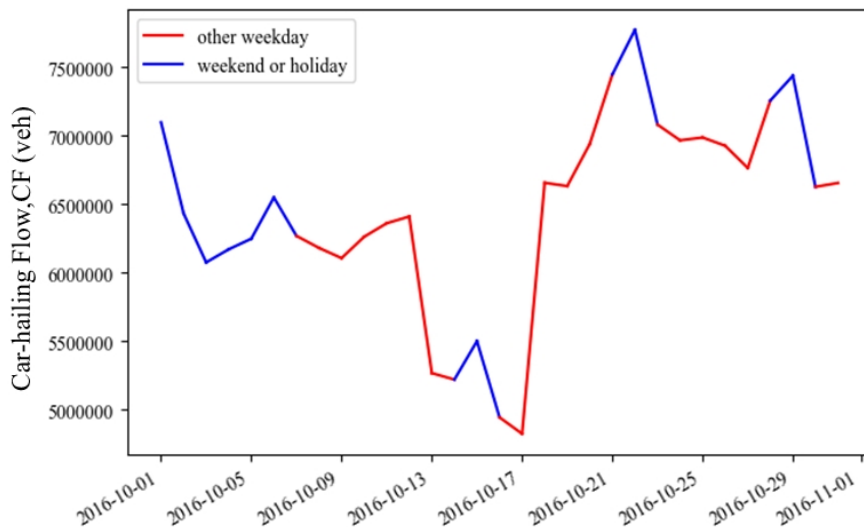


(f) Weekend (CF)

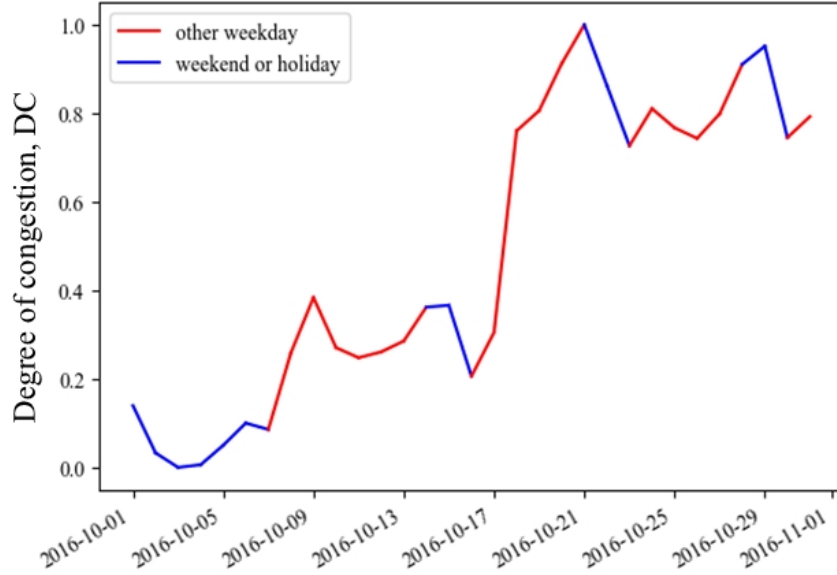
**Figure 3.** Degree of congestion (DC) and car-hailing Flow (CF) for different periods

In Figure 3(a-c), a bimodal distribution can be observed, and the congestion degree is low on the holiday (Figure 3(a)). The low level of congestion can be attributed to the following: (i) a large number of urban residents travel on vacation to other cities, relieving the daily traffic pressure in the central part of Chengdu; (ii) commuting peaks decrease during holidays and the travel time distribution on the network becomes homogeneous, thereby reducing the level of congestion. As for car-hailing flow in Figure 3(d-f), a ‘multi-peaks’ characteristic appears on holidays, weekdays, and weekends. Traffic states of these multi-peaks will switch on and off between the congestion and steady flow state (Kerner et al., 2007). And this ‘multi-peaks’ characteristic, unaffected by holidays or weekends, is triggered by increased demand for car-hailing services.

Notably, an interesting hierarchical structure appears in both DC and CF plots, except for holidays. The fitting index  $f^2$  also reveals this phenomenon mathematically.  $f^2$  of the two measurements are larger than 0.9 during holidays, while during other times, they range between 0.52 and 0.75. The hierarchical structure suggests that daily travel conditions exist a rather big fluctuation, whether for car-hailing or urban roads. Figure 4 depicts the total CF and average daily DC of the network, where the x-axis represents the date, and the y-axis represents the measurement value. The red and blue lines indicate measurements of weekdays and weekends or holidays, respectively.



(a) Total car-hailing flow per day



(b) Degree of congestion per day

**Figure 4.** Total daily CF and mean DC of the network

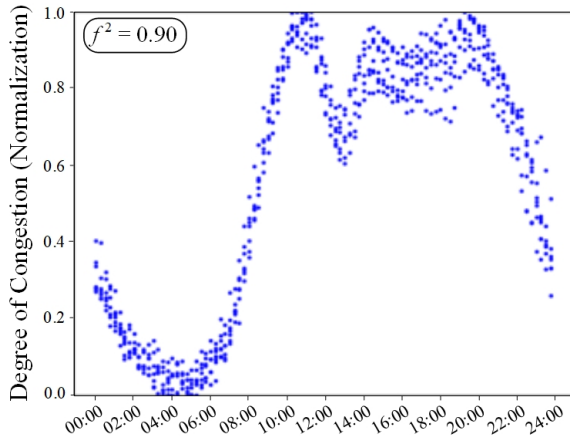
It can be seen from [Figure 4](#) that a flow drop (about 12<sup>th</sup> to 18<sup>th</sup> October) and a congestion degree rise (about 16<sup>th</sup> to 18<sup>th</sup> October) after the National Day holiday. As there were no extreme weather conditions and big public activities during this period, this may be the reason for the appearance of hierarchical structures. Following this step, a min-max normalization calculation is performed to eliminate the impact of fluctuation as follows:

$$x_N = \frac{x_j - \min(\mathbf{x}_{day})}{\max(\mathbf{x}_{day}) - \min(\mathbf{x}_{day})} \quad (7)$$

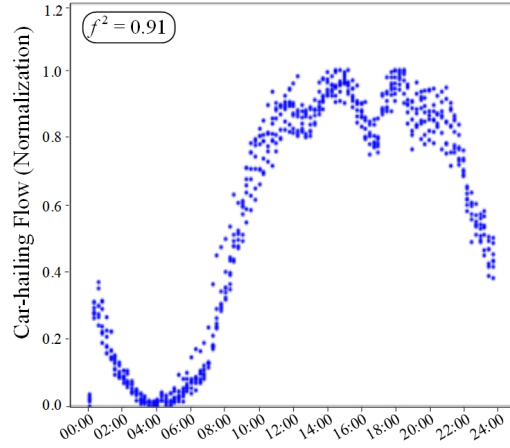
where,  $x_N$  is the min-max normalization value of  $x_j$  of sample interval  $j$ ;  $x_j$  is the original measurement value at sample interval  $j$ ;  $\mathbf{x}_{day}$  denote measurement value set of all sample intervals in a certain day.

The min-max normalization values of DC and CF, i.e., the DC-N and CF-N values, are illustrated in [Figure 5](#). In all scenarios, the hierarchical structures disappear, and the fitting index values reach quite a high level, at around 0.89~0.95. Consequently, we can deduce that the fluctuation of measurement values causes hierarchical structures. However, a crucial point still requires further explanation: what causes this fluctuation?

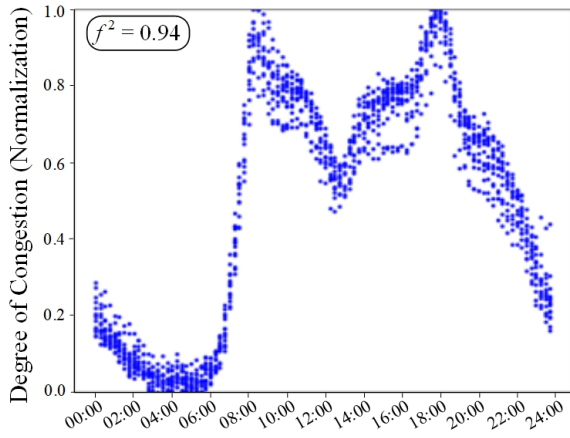




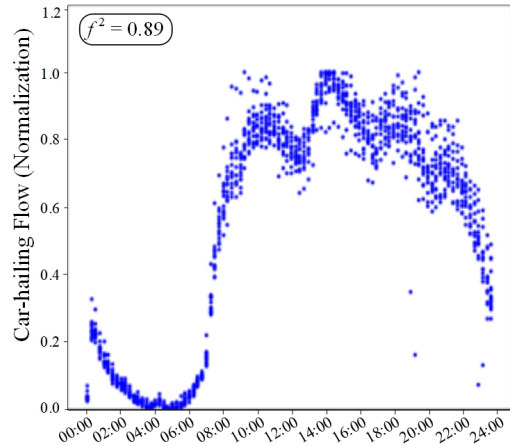
(a) National Day (DC-N)



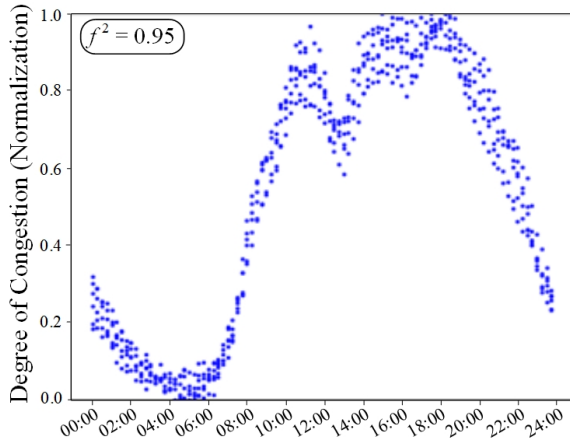
(d) National Day (CF-N)



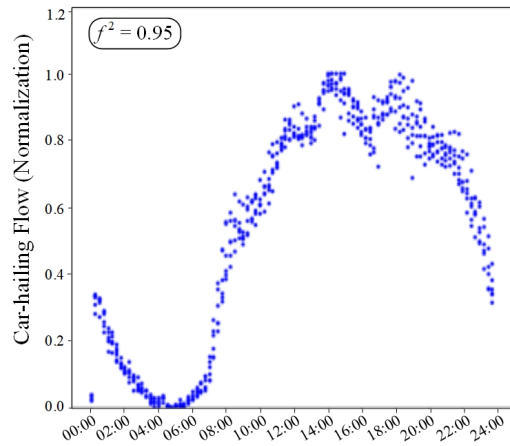
(b) Weekday (DC-N)



(e) Weekday (CF-N)



(c) Weekend (DC-N)



(f) Weekend (CF-N)

**Figure 5.** Daily car-hailing flow and INRIX score values (after normalization)

In terms of the general trend shown in [Figure 4](#), the degree of congestion remains low during holidays, while the car-hailing flow is at a rather high level. It demonstrates that car-hailing accounts for a bigger share of travel modes during holidays than usual, consistent with holiday travel behaviors. Therefore, the number of car-hailing vehicles decreases after the holidays, as car owners tend to accept car-hailing orders during the holidays and then rest **after the holidays** to maximize revenues. This number decline will lead to fluctuation and cause hierarchy. Regarding road traffic, the main reason is that companies shift vacations a few days before or back. Different companies will have various vacation shift schedules, resulting in a delayed increase in congestion degree. After approximately one week, daily traveling returns to normal, and traffic volume rises, generating fluctuations.

In conclusion, the car-hailing vehicle flow displays a ‘multi-peaks’ characteristic, resulting from service demands across multiple periods. This characteristic is somewhat diminished during holidays, suggesting that car-hailing vehicles are directly influenced by the alternation between workdays and holidays. Inferred from the estimated urban traffic speed data, the degree of congestion values exhibit a distinct bimodal characteristic. This is consistent with traffic flow features in traffic flow theory, thereby validating the effectiveness of the proposed estimation framework.

### ***5.2 Spatial pattern analysis***

By studying the spatial distribution of urban road traffic, we can identify congestion hotspots and help to improve traffic management. This section will investigate the spatial distribution of car-hailing vehicles and urban road traffic, as well as their relationships.

The formation and dissipation of car-hailing vehicle flow and urban road traffic congestion scores are observed hourly throughout National Day, weekdays, and weekends. Several critical transitional points are selected and displayed in [Figure 6](#). The label denotes the ratio to the maximal measurement values. [Figure 6\(a-d\)](#) depict the spatial distribution of car-hailing vehicles from 2-5 a.m., 7-8 a.m., 11-12 a.m., and 7-8 p.m., whereas [Figure 6\(e-h\)](#) depict the spatial distribution of urban road traffic of 2-5 a.m., 7-8 a.m., 9-10 a.m., and 9-10 p.m. It should be noted that a major difference between the two types of figures is that the heatmap of CF volumes is much sparser than that of DC, which is caused by the magnitude of measurement methods. The difference will not affect the main pattern of each type of heatmap.

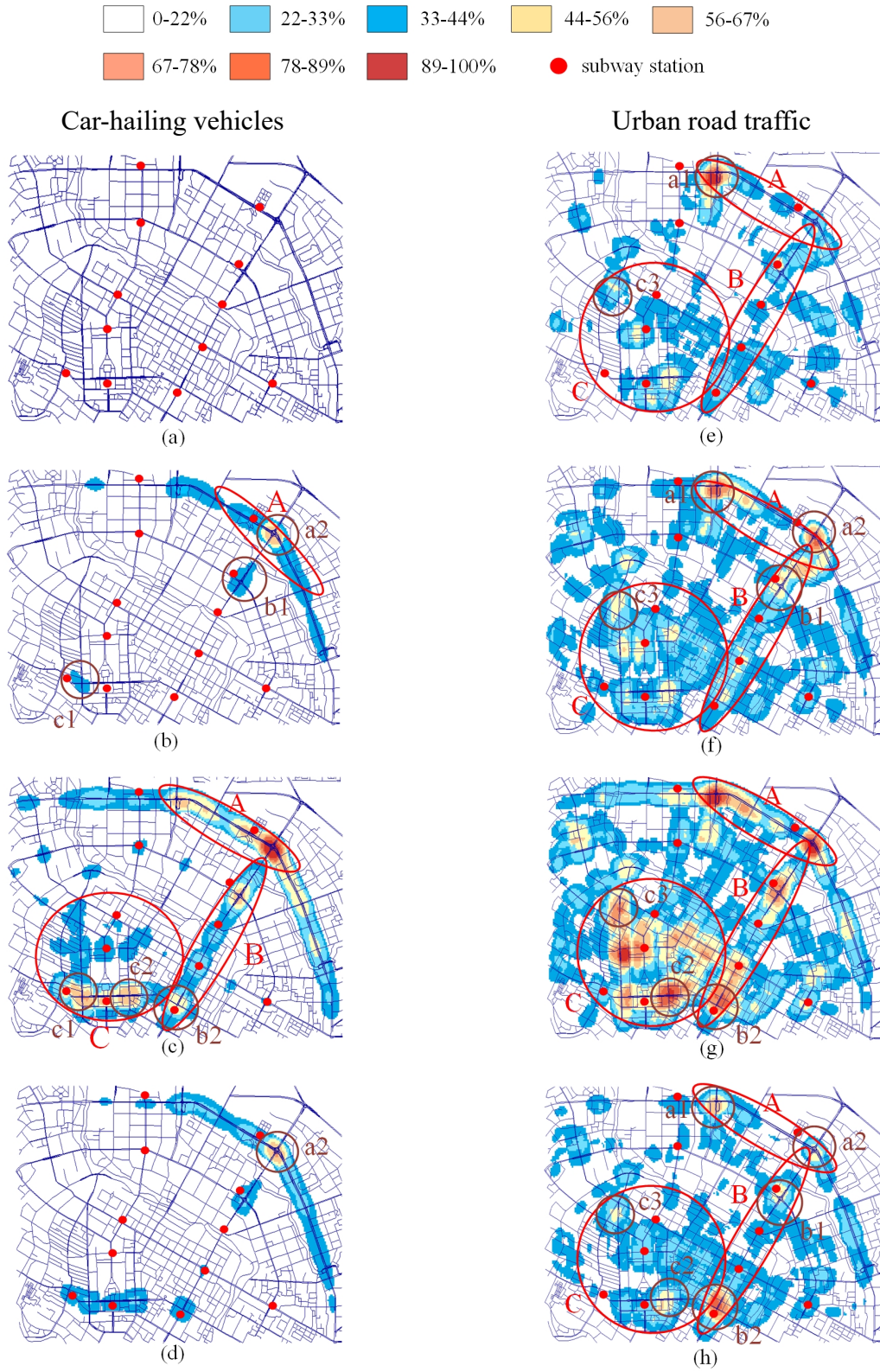


**Figure 6.** Spatial distribution of car-hailing vehicles and urban road traffic.

As in [Figure 6\(a\)](#), for CF volume, all roads are in low values. However, for the urban road traffic in [Figure 6\(e\)](#), the  $a1$  intersection in area  $A$  has a high congestion score. Several roads in areas  $A$ ,  $B$ , and  $C$  have relatively high congestion scores, with vehicles primarily concentrated around subway stations, which can be considered commercial centers.

The volume of CF increases gradually after 6 a.m., as demonstrated in [Figure 6\(b\)](#). Car-hailing vehicles congregate on the ring road of area  $A$ , with a high value at point  $a2$  and a moderate clustering at  $b1$ ,  $c1$ . For DC, the congestion in area  $A$  dissipates outward from  $a1$  and  $a2$  at 7 a.m., as depicted in [Figure 6\(f\)](#). Analogous, multiple subway stations located in areas  $B$  and  $C$  have relatively high congestion scores, which radiate from subway stations.

Since then, the number of car-hailing vehicles continued to increase, as shown in [Figure 6\(c\)](#). The high-value area of the ring road in area  $A$  continues to expand around  $a2$ , while new high-value clustering  $b2$  and  $c2$  appear in regions of  $B$  and  $C$ . Additionally, numerous intersections begin to exhibit clustering phenomena. This situation persists till 11 a.m. and is virtually unchanged from 12 a.m. to 7 p.m. After 7 p.m., the aggregation of car-hailing vehicles begins to dissipate slowly. As shown in [Figure 6\(d\)](#), the aggregation areas  $A$ ,  $B$ , and  $C$  shrink to  $a2$ ,  $b1$  and  $b2$ ,  $c1$ ,  $c2$ , respectively. The status will return to [Figure 6\(a\)](#) at around 2 a.m.

On the other hand, as urban road traffic congestion levels reach the peaks at 8 a.m., DC at  $b2$  and  $c2$  also grow significantly, as illustrated in [Figure 6\(g\)](#). Then the spatial distribution pattern can be divided into two categories: (i) from 9 a.m. to 6 p.m. on the holiday and weekends, the spatial distribution of DC is relatively stable; (ii) from 9 a.m. to 1 p.m. on weekdays, congestion gradually dissipates and forms the spatial distribution pattern depicted in [Figure 6\(f\)](#). DC values continue to increase till 6 p.m., and the traffic congestions in areas  $A$ ,  $B$  and  $C$  are still centered on neighbors of  $a2$ ,  $b1$  and  $b2$ ,  $c1$  and  $c2$ . Then, road congestion decreases, and at around 9 p.m., the spatial distribution pattern turns to the status shown in [Figure 6\(h\)](#). It will then revert to [Figure 6\(e\)](#) for the next day.

The aggregation areas of car-hailing vehicles are mainly located in three areas: the ring road of area  $A$ , the main streets of area  $B$ , and the large square area of the city center in area  $C$ . The aggregation points are  $a2$ ,  $b1$ , and  $c1$  before 11 a.m., while after 11 a.m.  $b2$  and  $c2$  emerge. Car-hailing vehicles tend to congregate around intersections and are impacted by the distribution of subway stations. As for urban traffic congestion, easy-to-congest areas are also in areas  $A$ ,  $B$ , and  $C$ . The aggregation point locates at  $a1$  before 5 a.m. During 5 and 9 a.m., vehicles congregate at

subway stations, and two new aggregation points,  $b2$  and  $c2$ , appear after 9 a.m. In addition, there is a modest aggregation at  $c3$ , although no significant congestion occurs.

In summary, while there are similarities between CF and DC heat maps, with shared hotspots in areas  $A$ ,  $B$ , and  $C$ , some differences also exist. Furthermore, the vehicle aggregation points for the two heatmaps exhibit a certain correlation: gathering around  $a2$ ,  $b1$ , and  $c1$  before morning peaks, and then generating two new points ( $b2$  and  $c2$ ).

## **6. Discussions on differences between car-hailing vehicles and urban traffic flow**

As car-hailing service has gradually occupied the market, GPS data of car-hailing service play an important role in providing information for ITS. Essentially, the generic framework proposed in this work can be easily employed in most cities owing to the popularity of car-hailing services. The effectiveness of the framework has been tested from experimental results. On the other hand, this also sheds light on mining differences between car-hailing vehicles and urban traffic patterns, which is one of the main contributions of this work.

### **6.1 Temporal differences**

Indeed, reliable assessments of urban traffic velocity can be made by GPS-enabled car-hailing services (Herrera et al., 2010). However, it does not imply that car-hailing vehicles and urban traffic patterns will be similar—they exhibit different diurnal forms. Differences can be seen from the result of temporal pattern analysis, as shown in Figure 3 and Figure 5. A general sample diagram of the two patterns is illustrated in Figure 7 for easy comparison.

In Figure 7, the y-axis is the dimensionless measurement values of CF and DC, while the x-axis is the time of the day. Note that the diurnal sample diagram is drawn according to the general shapes of DC and CF in Figure 3 and Figure 5. For car-hailing vehicles (CF, shown as orange dot-dash lines in Figure 7), additional peaks occur despite the two common peaks (morning and evening peaks, denoted as red arrows) as in urban traffic (DC, shown as blue lines in Figure 7). One is at around 2 p.m., and the other is at around 9 p.m., denoted as orange arrows. We regard these peaks as products of different travel behaviors of car-hailing vehicles: unlike common daily commute purposes, customers tend to employ car-hailing services in the early afternoon for entertainment purposes and at around 9 p.m. for returning home. The additional peaks in car-hailing services are the main points of difference compared to urban vehicle patterns in the temporal scope.

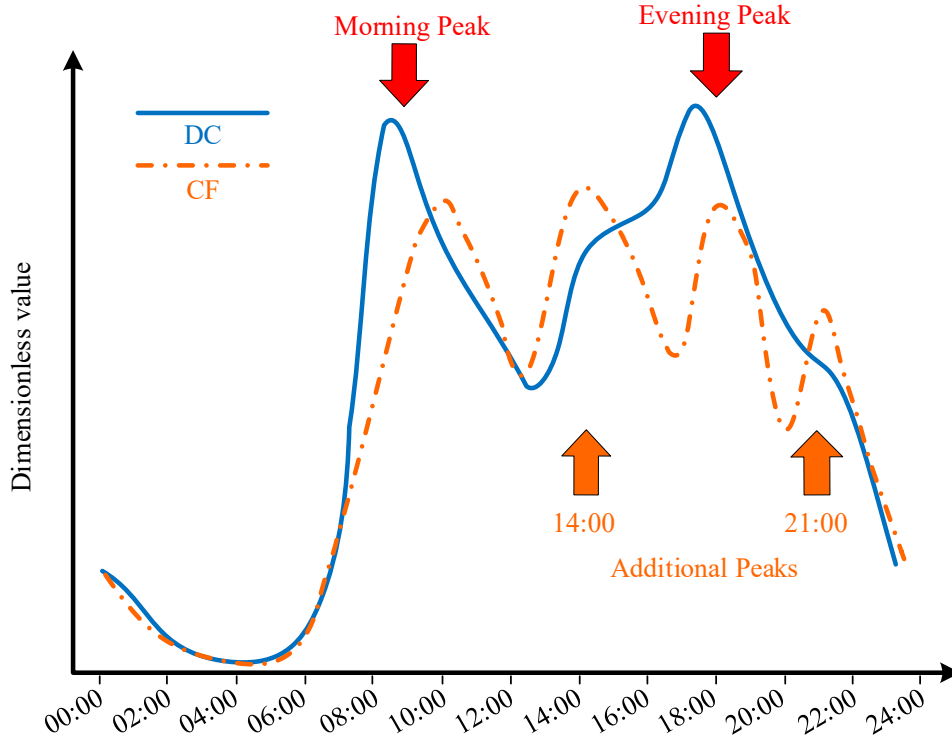


**Figure 7.** Temporal pattern comparison (diurnal sample)

### 6.2 Spatial differences

Regarding spatial scope, regardless of CF volumes or DC conditions, vehicles congregate at the same points, corresponding to the CBD or points of interest in Chengdu City. Nevertheless, differences still exist. As can be more clearly observed in [Figure 6\(a-d\)](#), car-hailing vehicles tend to travel along the ring roads to save time (the ring roads in Chengdu were designed as expressways). Moreover, [Figure 7](#) reveals that the morning and evening peaks for car-hailing services occur slightly later than those for urban traffic. This time delay might manifest as postponed spatial aggregation in the spatial domain, a factor that must be considered when estimating urban traffic patterns using car-hailing trace data.

### 6.3 Potential usage values

By its very nature, car-hailing vehicles are components of urban traffic flow, and there are intrinsic correlations between them. Understanding their differences in the temporal-spatial domain is crucial for developing effective management methods for transportation departments and operation approaches for car-hailing service providers. The proposed framework in this paper can simultaneously estimate the patterns of both car-hailing vehicles and urban traffic, enabling analysis of their temporal-spatial patterns for more flexible, reliable, and cost-effective urban

mobility. This analysis has demonstrated the differences between car-hailing services and urban traffic flow in the temporal-spatial domain, offering two main potential usage values.

First, understanding these differences can provide essential supplemental information for transportation management staff and policymakers. In the big-data era, the transportation department considers car-hailing service data a major data source that is cost-effective and easy to obtain compared to traditional sensor data. Comprehending the different patterns of car-hailing services and urban traffic flow, and distinguishing the collected car-hailing data from actual urban traffic, will contribute to a good grasp of transportation network conditions. Moreover, it can help transportation management staff and policymakers formulate more precise policies and methods to alleviate traffic congestion when provided with car-hailing data.

Second, understanding the difference can also facilitate a comparison of different travel modes and induce travelers to choose car-hailing services, such as Mobility as a Service (MaaS) (Wong et al., 2020) or Mobility-on-demand system (Fiedler et al., 2022). Urban traffic reflects private car conditions more, while car-hailing is another mode choice, a sharing economy (Barnes et al., 2020) that can reduce car ownership (Rayle et al., 2016). By leveraging the knowledge of the temporal-spatial difference between car-hailing vehicles and urban traffic, dispatching solutions or dynamic pricing policies for different periods and locations can be developed to offer better car-sharing mobility and attract more private car owners to use car-hailing services.

## **7. Conclusions**

This paper presents an easy-to-handle approach for estimating and analyzing urban traffic patterns using car-hailing vehicle trace data. The proposed framework integrates essential functionalities, and a congestion score calculation procedure based on the INRIX index is employed to describe the status of roads. The effectiveness of the framework is evaluated through experiments conducted with real-world car-hailing record data, and temporal-spatial distribution analyses are carried out based on the estimated car-hailing flow matrix and urban traffic congestion score matrix.

The experimental results demonstrate the proposed framework's effectiveness for estimating and analyzing urban traffic patterns. The findings reveal a 'multi-peaks' temporal distribution of car-hailing vehicle flow and a bimodal temporal distribution of road congestion status. Moreover, a hierarchical structure caused by holiday traffic fluctuations is discovered and explored in detail. Spatial distribution analyses show that the hotspots of car-hailing vehicles and urban traffic exhibit spatial convergence and relative consistency in vehicle aggregations. The findings on temporal-

spatial distribution patterns offer insights into investigating the relationships between car-hailing vehicles and urban traffic, and evaluating the effects of holidays on urban traffic patterns. This work also highlights the potential contributions of analyzing different patterns in car-hailing vehicles and urban traffic.

Future studies will be conducted with more data input from other cities. Using different car-hailing service data to verify the ‘multi-peaks’ phenomenon and discussing the pattern differences between car-hailing service and urban traffic will be of great practical significance for transportation departments and car-hailing service providers. Also, it will be worth discussing the influence mechanism of penetration rates (car-hailing vehicles to normal vehicles) on estimation accuracy. Moreover, a specific method to enhance the incomplete estimated tensor will be a promising way for future research.

### **Acknowledgments**

This work is supported by the Science and Technology Project of Sichuan Province under Grant 2020YFSY0020. Weike Lu is supported by the National Natural Science Foundation of China under Grant 62103292. Tianli Tang is supported by the project of Jiangsu Funding Program for Excellent Postdoctoral Talent.

### **Author Contributions**

The authors confirm their contribution to the paper as follows: study conception and design: J. Mao, K. Yang, L. Liu; data collection: J. Mao, H. Huang, and W. Lu; analysis and interpretation of results: J. Mao, H. Shi, and H. Huang; draft manuscript preparation: J. Mao, H. Shi, T. Tang. All authors reviewed the results and approved the final version of the manuscript.

### **Disclosure statement**

The authors declare that they have no known competing financial interests or personal relationships that could have appeared to influence the work reported in this paper.

### **References**

- Al-Dohuki, S., Wu, Y., Kamw, F., Yang, J., Li, X., Zhao, Y., Ye, X., Chen, W., Ma, C., & Wang, F. (2016). Semantictraj: A new approach to interacting with massive taxi trajectories. *IEEE transactions on visualization and computer graphics*, 23(1), 11-20.
- An, S., Yang, H., & Wang, J. (2018). Revealing recurrent urban congestion evolution patterns with taxi trajectories.



- ISPRS International Journal of Geo-Information*, 7(4), 128.
- An, S., Yang, H., Wang, J., Cui, N., & Cui, J. (2016). Mining urban recurrent congestion evolution patterns from GPS-equipped vehicle mobility data. *Information Sciences*, 373, 515-526.
- Barnes, S. J., Guo, Y., & Borgo, R. (2020). Sharing the air: Transient impacts of ride-hailing introduction on pollution in China. *Transportation Research Part D: Transport and Environment*, 86, 102434.
- Chen, X., He, Z., & Sun, L. (2019). A Bayesian tensor decomposition approach for spatiotemporal traffic data imputation. *Transportation Research Part C: Emerging Technologies*, 98, 73-84.
- Correa, D., & Ozbay, K. (2022). Urban path travel time estimation using GPS trajectories from high-sampling-rate ridesourcing services. *Journal of Intelligent Transportation Systems*, 1-16.
- D'Andrea, E., & Marcelloni, F. (2017). Detection of traffic congestion and incidents from GPS trace analysis. *Expert Systems with Applications*, 73, 43-56.
- Deng, Y., Wang, J., Gao, C., Li, X., Wang, Z., & Li, X. (2021). Assessing temporal-spatial characteristics of urban travel behaviors from multiday smart-card data. *Physica A: Statistical Mechanics and its Applications*, 576, 126058.
- Dong, W., Wang, Y., & Yu, H. (2019). An identification model of critical control sub-regions based on macroscopic fundamental diagram theory. *ITS Journal*, 23(1/6), 441-451.
- Fiedler, D., Čertický, M., Alonso-Mora, J., Pěchouček, M., & Čáp, M. (2022). Large-scale online ridesharing: the effect of assignment optimality on system performance. *Journal of Intelligent Transportation Systems*, 1-22.
- Gade, K. (2010). A non-singular horizontal position representation. *The journal of navigation*, 63(3), 395-417.
- He, Z., Hu, J., Park, B. B., & Levin, M. W. (2019). Vehicle sensor data-based transportation research: Modeling, analysis, and management (Vol. 23, pp. 99-102). Taylor & Francis.
- Herrera, J. C., Work, D. B., Herring, R., Ban, X. J., Jacobson, Q., & Bayen, A. M. (2010). Evaluation of traffic data obtained via GPS-enabled mobile phones: The Mobile Century field experiment. *Transportation Research Part C: Emerging Technologies*, 18(4), 568-583.
- Kerner, B. S., Klenov, S. L., & Hiller, A. (2007). Empirical test of a microscopic three-phase traffic theory. *Nonlinear Dynamics*, 49(4), 525-553.
- Lasley, P. (2021). *2021 Urban Mobility Report*. T. A. M. T. Institute
- Liu, Y., Jia, R., Ye, J., & Qu, X. (2022). How machine learning informs ride-hailing services: A survey. *Communications in Transportation Research*, 2, 100075.
- Liu, Y., Liu, Z., Vu, H. L., & Lyu, C. (2020). A spatio-temporal ensemble method for large-scale traffic state prediction. *Computer-Aided Civil and Infrastructure Engineering*, 35(1), 26-44.
- Lyman, K., & Bertini, R. L. (2008). Using travel time reliability measures to improve regional transportation planning and operations. *Transportation research record*, 2046(1), 1-10.
- Moreira-Matias, L., Gama, J., Ferreira, M., Mendes-Moreira, J., & Damas, L. (2013). Predicting taxi-passenger demand using streaming data. *IEEE Transactions on Intelligent Transportation Systems*, 14(3), 1393-1402.
- Qian, C., Li, W., Duan, Z., Yang, D., & Ran, B. (2021). Using mobile phone data to determine spatial correlations between tourism facilities. *Journal of Transport Geography*, 92, 103018.
- Rao, A. M., & Rao, K. R. (2012). Measuring urban traffic congestion-a review. *International Journal for Traffic & Transport Engineering*, 2(4).
- Rayle, L., Dai, D., Chan, N., Cervero, R., & Shaheen, S. (2016). Just a better taxi? A survey-based comparison of taxis, transit, and ridesourcing services in San Francisco. *Transport Policy*, 45, 168-178.
- Reed, T. (2019). *Inrix global traffic scorecard* (Available: <http://inrix.com/scorecard>)
- Tu, W., Xiao, F., Li, L., & Fu, L. (2021). Estimating traffic flow states with smart phone sensor data. *Transportation Research Part C: Emerging Technologies*, 126, 103062.
- Wong, Y. Z., Hensher, D. A., & Mulley, C. (2020). Mobility as a service (MaaS): Charting a future context. *Transportation Research Part A: Policy and Practice*, 131, 5-19.
- Xing, J., Wu, W., Cheng, Q., & Liu, R. (2022). Traffic state estimation of urban road networks by multi-source data fusion: Review and new insights. *Physica A: Statistical Mechanics and its Applications*, 127079.
- Yu, J., Stettler, M. E., Angeloudis, P., Hu, S., & Chen, X. M. (2020). Urban network-wide traffic speed estimation with massive ride-sourcing GPS traces. *Transportation Research Part C: Emerging Technologies*, 112, 136-152.
- Yu, W. (2018). Discovering frequent movement paths from taxi trajectory data using spatially embedded networks and association rules. *IEEE Transactions on Intelligent Transportation Systems*, 20(3), 855-866.
- Yu, W., Dongbo, Z., & Yu, Z. (2022). GPS data mining at signalized intersections for congestion charging. *Computational Economics*, 59(4), 1713-1734.
- Yuan, Y., Zhang, W., Yang, X., Liu, Y., Liu, Z., & Wang, W. (2021). Traffic state classification and prediction based on trajectory data. *Journal of Intelligent Transportation Systems*, 1-15.

- Zheng, Y. (2015). Trajectory data mining: an overview. *ACM Transactions on Intelligent Systems and Technology (TIST)*, 6(3), 1-41.
- Zhong, G., Wan, X., Zhang, J., Yin, T., & Ran, B. (2016). Characterizing passenger flow for a transportation hub based on mobile phone data. *IEEE Transactions on Intelligent Transportation Systems*, 18(6), 1507-1518.